

Electroweak baryogenesis from charged current anomalies in B meson decays

Peter Athron,^{1,*} Michael J. Ramsey-Musolf,^{2,3,4,5,†} Cristian Sierra,^{1,2,‡} and Yongcheng Wu^{1,§}

¹*Department of Physics and Institute of Theoretical Physics,*

Nanjing Normal University, Wenyuan Road, Nanjing, Jiangsu, 210023, China

²*Tsung-Dao Lee Institute & School of Physics and Astronomy, Shanghai Jiao Tong University, Shanghai 200240, China*

³*Shanghai Key Laboratory for Particle Physics and Cosmology, Key Laboratory for Particle Astrophysics and Cosmology (MOE), Shanghai Jiao Tong University, Shanghai 200240, China*

⁴*Amherst Center for Fundamental Interactions, Department of Physics, University of Massachusetts, Amherst, MA 01003, USA*

⁵*Kellogg Radiation Laboratory, California Institute of Technology, Pasadena, CA 91125, USA*

(Dated: February 3, 2025)

We demonstrate for the first time that new physics explaining the long standing charged B meson anomalies, $R(D^{(*)})$, can be the source of CP violation that explains the observed baryon asymmetry of the universe (BAU). We consider the general two Higgs doublet model with complex Yukawa couplings and compute the BAU in the semiclassical formalism, using a novel analytic approximation for the latter. After imposing constraints from both flavor observables and the electron electric dipole moment (eEDM), we find that a significant BAU can still be generated for a variety of benchmark points in the parameter space, assuming the occurrence of a sufficiently strong first order electroweak phase transition. These scenarios, which explain both the $R(D^{(*)})$ flavor anomalies and the BAU, can be probed with future eEDM experiments and Higgs factories measurements.

Introduction. The origin of the observed baryon asymmetry of the Universe (BAU) is one of the deepest puzzles in particle physics and cosmology. To generate it, the Sakharov conditions [1] must be satisfied: (1) baryon number violation; (2) C and CP violation and (3) departure from thermal equilibrium. The Standard Model (SM) in principle can fulfill all three conditions, but in practice fails to do so for the latter two. Thus, successful baryogenesis requires physics beyond the SM (BSM).

One of the most attractive mechanisms for this is Electroweak Baryogenesis (EWBG) [2–6] as it can be tested with electric dipole moments (EDMs) [7], collider physics [8, 9] and gravitational waves [10–12]. EWBG requires new bosonic degrees of freedom in order to generate a strong first order phase transition (SFOPT) that breaks electroweak symmetry when the Higgs field develops a non-zero vacuum expectation value (VEV). In the SFOPT bubbles of the broken phase nucleate and expand. Non-perturbative electroweak sphaleron processes that change total baryon plus lepton number [13, 14] (condition 1) are active outside the bubbles but heavily suppressed inside. The presence of the phase transition and the associated phase boundary (bubble wall) reflect a departure from equilibrium (condition 3). CP violating interactions (condition 2) at the bubble wall generate a chiral asymmetry, i.e., a non zero number density for left handed particles. This asymmetry generated at the bubble wall subsequently diffuses into the space outside it. The sphaleron process then converts that chiral asymmetry into a baryon asymmetry that is not washed out when the corresponding particles are swept inside the bubble wall as it expands.

A BAU compatible with observation can only be pre-

dicted if new sources of CP violation are present in the BSM model. In this work we show that this new CP violation may be sourced from interactions that have been proposed [15–17] to solve an entirely different problem: long standing and widely considered deviations between SM predictions and the data in flavor physics experiments. Specifically, the $R(D^{(*)})$ ratios in $b \rightarrow c\tau\nu$ decays [18] and the angular observables in $b \rightarrow s\mu^+\mu^-$ transitions [19, 20] in B meson decays, also known as the charged and neutral current anomalies respectively, have garnered considerable attention in flavor physics analyses [21–23]. Experimental measurements of these observables deviate from SM predictions by roughly 3σ and by more than 5σ when considering global fits to all $b \rightarrow s\mu^+\mu^-$ data [21, 22]. Here we investigate the link between the BAU and these persistent signals in the measurements from the LHCb and other particle detectors.

We show for the first time that the charged current anomalies could be revealing new physics that gives rise to a successful EWBG mechanism. This mechanism generates the observed BAU while satisfying EDM [24], flavor and theoretical constraints [16, 17]. Several attempts at linking flavor anomalies to the BAU have been presented in the literature [25–29], but none of them have considered the effects in the BAU from new CP-violating couplings entering in the charged current anomalies [15–17]. To establish the flavor anomaly-BAU connection, we employ the semi-classical formalism also called Wentzel-Kramers-Brillouin (WKB) method for a leptonic CP-violating source, which provides a more conservative estimate than other approaches [30] as discussed below.

For concreteness, we adopt the general two Higgs doublet model (G2HDM), which includes complex leptonic

Yukawas and extra bosonic degrees of freedom. The latter can modify the shape of the Higgs potential away from that of the SM, wherein electroweak symmetry is broken only through a smooth cross-over transition [31]. As a result it has been found both perturbatively [32–41] and non-perturbatively [36, 37] that the electroweak phase transition in the 2HDM can be strongly first order.

EWBG in the 2HDM has been studied extensively with both scalar [27, 41–51] and fermion sources [25, 52–56] constrained by flavor physics, but here we compute the BAU from a source that also explains the charged current anomalies. Furthermore, we fit the observed BAU and the flavour anomalies while simultaneously explaining another recent (local) 3σ excess in searches for $t \rightarrow b H^+ \rightarrow b \bar{b} c$ from the ATLAS experiment [57] that have been linked to the B meson anomalies in Ref. [16]. Finally, we show that these scenarios can be probed at future Higgs factories [58, 59].

Electroweak baryogenesis. The dynamics governing the generation of the left-handed fermion number density n_L entails three elements: CP-violating scattering at the bubble wall; particle number density transfer reactions; and diffusion. The corresponding equations that encode these dynamics follow from the general set of Kadanoff-Baym (KB) equations. Solving the full set of KB equations is practically challenging, and various approximations have been taken in the literature. Here, we follow the WKB treatment of Refs. [60–62] that yields a set of Boltzmann equations which one may further reduce to a tractable diffusion equation for n_L .

For the present purposes, a further simplification follows from the work of Ref. [63]. The CP-violating source we consider resides in the lepton Yukawa sector of the G2HDM. The associated CP-conserving Yukawa interactions will re-distribute the lepton asymmetry among the left- and right-handed leptons and Higgs particles. Quark Yukawa interactions will then re-distribute the Higgs number density into the left- and right-handed quark number densities. Strong sphaleron processes will lead to further rebalancing between the left- and right-handed quark densities. Thus, to obtain the resultant left-handed number density relevant to weak sphaleron processes, one must solve a set of coupled Boltzmann equations for the Higgs density and left- and right-handed lepton and quark densities. For a detailed discussion in the case of lepton-mediated EWBG, see Ref. [53]. In practice, for this case the authors of Ref. [63] find that $n_L(x)$ can be dominated by the density of left-handed leptons, $l_L(x)$, so that to an order ten percent level of accuracy, one may consider a single Boltzmann equation for $l_L(x)$. Following the prescription of Refs. [60–62] in the WKB formalism and using the diffusion approximation, one then obtains the single species diffusion equation

$$\bar{D}_l l''(z) + v_w l'(z) + \bar{\Gamma}_l l(z) = \bar{S}_l, \quad (1)$$

where we have dropped the the subscript “ L ” for simplicity. Here, v_w denotes the bubble wall velocity and \bar{D}_l the effective diffusion constant which is proportional to the diffusion coefficient D_l (expressing how the particles spread out), with modifications to account for the effect of non-zero v_w ; $\bar{\Gamma}_l$ is the modified collision rate from in-elastic scattering with the wall; and \bar{S}_l is the CP-violating source term. Within the WKB method, the latter arises at second order in derivatives. On the other hand, in the VEV resummation (VR) framework [30, 64, 65], the source term is first order in derivatives, so we expect our approach to result in conservative (under-)estimates of the BAU. For the explicit expressions for all the terms in Eq.(1) the reader is referred to the End Matter, Eq.(A1).

We now comment further on the assumptions leading to the aforementioned simplified treatment. First, the lepton Yukawa interactions are sufficiently slow that the transfer of lepton number densities into other species is relatively inefficient [63]. The diffusion equations for both right-handed and left-handed leptons can be simplified into a single equation that decouples from both quarks and the Higgs boson, the latter because of the slow lepton Yukawa rate Γ_{Y_τ} as shown in Ref. [63]. Second, we take the left- and right-handed diffusion constants to be approximately equal: $D_l \equiv D_L = D_R \simeq 100/T$, which implies $l \equiv l_L = -\tau_R$. This was proven to be valid up to a 10% difference with respect to the exact treatment of having different diffusion constants, both analytically and numerically [63]. Given that $\bar{\Gamma} \gg v_w^2/D_l$, Eq.(1) can be solved analytically using the Green’s function method. We neglect the bubble wall curvature and work in the bubble wall rest frame, $z = |\mathbf{x} + \mathbf{v}_w t|$ and we take $z < -L_w/2$ as the symmetric phase, where L_w is the bubble wall thickness. In this way, the solution to Eq.(1) is given by [53, 63, 66–69]

$$l(z) = -\mathcal{A} e^{z \gamma_+^*}, \quad (2)$$

with the amplitude \mathcal{A} given in Eq.(A5).

The net baryon number density n_B is determined by solving the baryon number diffusion equation [70],

$$n_B''(z) - \frac{v_w}{D_q} n_B'(z) = \frac{\Gamma_{ws}}{D_q} \left(\mathcal{R} n_B(z) + \frac{3}{2} n_L(z) \right), \quad (3)$$

with $D_q = 7.2/T$ [71] the quark diffusion constant, $\Gamma_{ws} = 6.3 \times 10^{-6} T$ the electroweak sphaleron rate [72] and $\mathcal{R} = 15/4$ is the SM relaxation term. Here, the diffusion of the baryon density is sourced by the left-handed leptons $n_L(z) \simeq l(z)$ from Eq.(2) and the solution of Eq. (3) is given in terms of the ratio $Y_B \equiv n_B/s$ [70],

$$Y_B = -\frac{3\Gamma_{ws}}{2s} \frac{1}{D_q \lambda_+} \int_{-\infty}^{-L_w/2} l(z) e^{-\lambda_- z} dz, \quad (4)$$

where $s = (2\pi^2/45)g_* T^3$ is the entropy density at the temperature T , $g_* = 110.75$ are the degrees of freedom in

the G2HDM and $\lambda_{\pm} = 1/2D_q (v_w \pm \sqrt{v_w^2 + 4\mathcal{R}\Gamma_{ws}D_q})$. **Hints from flavor Physics.** Lepton flavor universality (LFU) is a fundamental feature of the SM and states that the W boson couples equally to the three lepton generations. It can be tested experimentally by considering ratios of semileptonic B meson decays to τ and light leptons l (either e or μ) defined as

$$R(D^{(*)}) = \frac{\text{BR}(\bar{B} \rightarrow D^{(*)}\tau\bar{\nu})}{\text{BR}(\bar{B} \rightarrow D^{(*)}l\bar{\nu})}, \quad (5)$$

with the latest experimental world average given by $R(D) = 0.342 \pm 0.026$, $R(D^*) = 0.287 \pm 0.012$ [73]. This implies a deviation of 3.2σ from the SM, thus motivating BSM physics in order to fit it. These ratios can be explained at tree level using complex lepton Yukawa couplings in the G2HDM while simultaneously satisfying all other flavor constraints at the 1σ level [15–17]. Explicitly, using the form factors provided by SuperIso 4.1 [74–78], we compute the G2HDM contributions to $R(D)$ and $R(D^*)$ as,

$$R(D) = \frac{1 + 1.73 \text{Re}(g_S^{\tau\tau}) + 1.35 \sum |g_S^{\ell\tau}|^2}{3.27 + 0.57 \text{Re}(g_S^{\mu\mu}) + 4.8 \sum |g_S^{\ell\mu}|^2}, \quad (6)$$

$$R(D^*) = \frac{1 + 0.11 \text{Re}(g_P^{\tau\tau}) + 0.04 \sum |g_P^{\ell\tau}|^2}{4.04 + 0.08 \text{Re}(g_P^{\mu\mu}) + 0.25 \sum |g_P^{\ell\mu}|^2}, \quad (7)$$

with $\ell = e, \mu, \tau$ and the scalar and pseudoscalar couplings $g_{S,P}^{\ell\ell'}$ given at tree level in Refs. [17, 79]. The latter are functions of the Yukawa textures with the complex phase θ defined in Eq.(C2) in the End Matter.

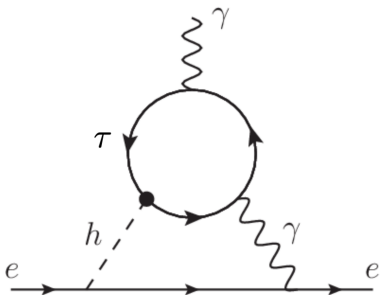


FIG. 1. Dominant two-loop Barr-Zee diagram with a τ lepton in the loop entering in the e EDM calculation.

We explore the possibility that complex phase θ can be large enough to explain the BAU, with the real and imaginary parts of the Yukawa couplings in Eq. (C2) still accommodating the aforementioned $R(D)$ and $R(D^*)$ results and EDM constraints. Regarding the latter, the Higgs fermion effective Lagrangian can be written as [80, 81],

$$-\mathcal{L}_{h\tau\tau} = \frac{m_\tau}{v} (\kappa_\tau \bar{\tau}\tau + i\tilde{\kappa}_\tau \bar{\tau}\gamma_5\tau) h, \quad (8)$$

allowing a matching between this effective theory and the G2HDM (see End Matter, Eq.(B3) for the relevant part of the G2HDM Lagrangian), obtaining

$$\begin{aligned} \kappa_\tau &= -\frac{\sin\alpha}{\cos\beta} + \frac{c_{\beta-\alpha}}{\cos\beta} \text{Re}(N_{\tau\tau}), \\ \tilde{\kappa}_\tau &= \frac{c_{\beta-\alpha}}{\cos\beta} \text{Im}(N_{\tau\tau}), \end{aligned} \quad (9)$$

where the CP-violating coupling $\tilde{\kappa}_\tau$ is given in terms of $\text{Im}(N_{\tau\tau}) = v \text{Im}(J_A)/(\sqrt{2}y_{\tau\tau}m_\tau)$, and J_A is the Jarlskog invariant defined in Eq.(C5) in the End Matter. The CP-conserving coupling κ_τ governs the Higgs signal strength that is relevant for future Higgs factories. It is written here in terms of $\text{Re}(N_{\tau\tau}) = v(\mu_{12} \text{Re}(J_A) - \mu_{11}y_{\tau\tau}^2)/(\sqrt{2}y_{\tau\tau}m_\tau\mu_{12}^{\text{HB}})$, with μ_{11} , μ_{12} and μ_{12}^{HB} being quadratic scalar couplings also defined in the End Matter below Eq.(C5).

Note that $\tilde{\kappa}_\tau$ directly contributes to both the electron EDM $|d_e|$ and also to the light quark EDMs through the two-loop Barr-Zee diagram in Fig. 1, which is proportional to the corresponding fermion mass (m_e or m_q). The light quark EDMs can further contribute to the neutron EDM (nEDM) with $\mathcal{O}(1)$ coefficient [82–85]. Therefore the contribution of the CP-violating coupling $\tilde{\kappa}_\tau$ to both the eEDM and nEDM could be comparable at first. However, the latest experimental measurements give $|d_e| < 4.1 \times 10^{-30}$ ecm [24] and $|d_n| < 1.8 \times 10^{-26}$ ecm [86] at 90% C.L., which differ by about 4 orders of magnitude. Hence, the eEDM will provide the dominant constraint in our scenario.

Comparing to the results of Ref. [87] for a τ lepton in the upper loop of the two-loop Barr-Zee diagram, the latest experimental measurement of the eEDM provides $|\tilde{\kappa}_\tau| \lesssim 0.078$. Regarding the future sensitivity on the eEDM, the next generation ACME III experiment will improve it by another order of magnitude to $\delta d_e \approx 4 \times 10^{-31}$ ecm [88], which provides then $|\tilde{\kappa}_\tau| \lesssim 0.0078$. In addition, the lepton Yukawa couplings will be further constrained by other B decays related to the neutral current anomalies, as well as from kinetically allowed Higgs flavor violating decays like $h \rightarrow \ell\ell'$ and lepton flavor violating decays of the form $\ell \rightarrow \ell'\gamma$ for $\ell, \ell' = e, \mu, \tau$ [16, 17, 79, 89].

Results. We now demonstrate that the G2HDM Yukawas shown by global fits to explain the $R(D^{(*)})$ anomalies and all other relevant constraints, can source sufficient CP violation to also explain the BAU. We find solutions that can do this while satisfying all the flavor constraints discussed above, as well as unitarity, stability and perturbativity bounds and constraints from electroweak precision observables via the S , T and U parameters [90]. The global fit was obtained by running GAMBIT [91–95] with SuperIso 4.1 [76–78], 2HDMC 1.8 [96] and HEPLike [97]. The scan follows the analysis of Ref. [17], specifically the scans around BM3 (originally defined in Ref. [16]) with all the likelihoods included there plus

a new likelihood introduced here for the eEDM from the JILA-NIST group bound on $|d_e|$ [24].

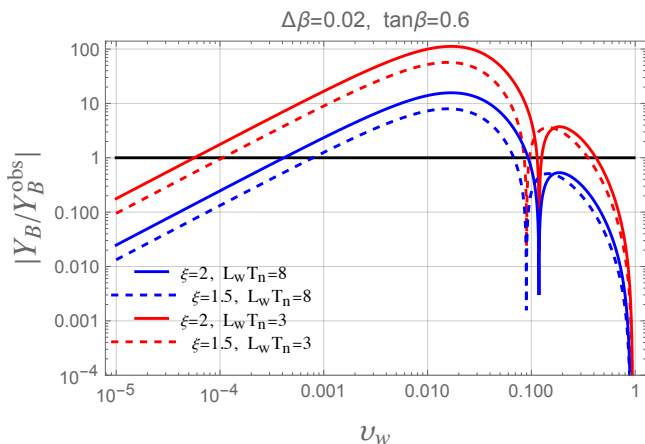


FIG. 2. Ratio $|Y_B/Y_B^{\text{obs}}|$ as a function of v_w with fixed values of the extra Yukawa couplings from the best fit point of the BM3 study of [17], $y_{\mu\mu} = 0.001$, $y_{\mu\tau} = 0.01$, $y_{\tau\tau} = 0.05$, $\theta = 2.15$ and $c_{\beta-\alpha} = 0.01$.

To determine the BAU from Eq.(4), we need to know the values of the so-called thermal parameters, quantities that characterize the first order phase transition. These thermal parameters can be determined from the fundamental G2HDM parameters in the Higgs potential, see Refs. [39–41] for recent studies. Here we simply select reasonable choices for the thermal parameters based both on previous work [39–41] and an understanding of how they influence the BAU calculation. We leave determining the underlying parameters in the Higgs potential that give rise to these thermal parameters, and showing how varying the Higgs potential parameters influences the BAU, to future work.

For all scenarios we fix $\Delta\beta = 0.02$ which is the maximum variation of the angle β in the field profiles (see Eq. (C1) in the End Matter). This is near the middle of the range of $\log(\Delta\beta)$ values generated for Ref. [41] and values of this order are relatively common amongst the points sampled there. We obtain the source term on the right hand side of Eq. (3) using the expressions given in the End Matter (see in particular Eqs. (A1) and (C6)). We then compute the analytical chiral lepton-antilepton asymmetry in Eq. (2) and proceed to numerically determine the BAU for different choices of the bubble wall velocity v_w , the bubble wall thickness, L_w , and the ratio $\xi \equiv v_n/T_n$, where T_n is the nucleation temperature and v_n is the electroweak VEV at T_n , and we simply fix $v_n = 200$ GeV in all scenarios since our results are really only sensitive to the ratio ξ .

First we consider the BAU that can be obtained for the best fit point from the global fit. Fig. 2 shows the BAU (specifically Y_B/Y_B^{obs} with $Y_B^{\text{obs}} = 8.59 \times 10^{-11}$ being the central value given by the Planck Collaboration [98])

plotted against the bubble wall velocity for different values of parameters characterizing the phase transition. The dashed (solid) curves are plotted for $\xi = 1.5$ (2), with the red versions for $L_w T_n = 3$, and the blue versions for $L_w T_n = 8$. These show that successful EWBG is achieved with a wide range of bubble wall velocities for a sufficiently SFOPT $\xi \gtrsim 1.5$ and relatively thin bubble wall widths $L_w T_n \gtrsim 3$, where the WKB approximation is still valid. The sharp dip in the BAU near $v_w = 0.1$ in Fig. 2 is due to cancellations between terms with different signs in the WKB calculation [61, 71].

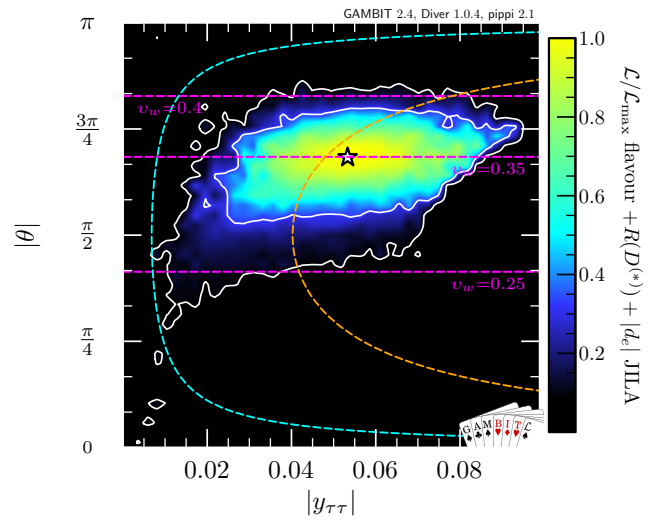


FIG. 3. Profile likelihood ratios $\mathcal{L}/\mathcal{L}_{\text{max}}$ from all flavor constraints in [16] and the JILA-NIST bound on $|d_e|$ [24]. The white star denotes the best fit point and white contours around it are the 1σ and 2σ confidence intervals. Overlaid on top of this are magenta horizontal dashed lines showing results for the BAU (using best fit values of the parameters from the global fit) for different values of v_w . These correspond to $Y_B/Y_B^{\text{obs}} = 1$ with $\xi = 1.5$ and $L_w T_n = 3$. The orange dashed line is the sensitivity projection for $|\tilde{\kappa}_\tau/\kappa_\tau|$ related to the CP-violating Yukawa coupling measurement from both the CEPC and the FCC-ee. The cyan dashed curve is the future sensitivity on the eEDM at the ACME III experiment [88].

In Fig. 3 we plot global fitting results that show solutions for the BAU coinciding with the allowed region that explains the flavor anomalies in the $|y_{\tau\tau}| - |\theta|$ plane of the G2HDM. The function \mathcal{L} on the colour bar is the sum of all flavor and eEDM likelihoods defined in GAMBIT and is normalized with respect to the maximum likelihood obtained over the parameter space of the G2HDM. The mass of the charged Higgs boson m_{H^\pm} mediating the tree level exchange $b \rightarrow c\tau\nu_l$ has been fitted close to 130 GeV, matching the local excess in searches for $t \rightarrow bH^+ \rightarrow b\bar{b}c$ with a local significance of 3σ as reported by the ATLAS experiment [57]. Furthermore, regarding constraints from the B_c meson lifetime, the fit gives $\text{BR}(B_c \rightarrow \tau\bar{\nu}) \leq 60\%$ for all sampling points and

30% at the best fit point value, which is within the current theoretical estimates according to Ref. [99].

Fixing $\xi = 1.5$ and $L_w T_n = 3$ and all Yukawa couplings to the best fit value obtained in the global fit, we also draw in Fig. 3 contours of $Y_B/Y_B^{\text{obs}} = 1$ for different bubble wall velocities (dashed magenta lines). We can see that successful EWBG can be achieved while satisfying all flavor constraints and the best fit value predicts $v_w = 0.35$ for $|\theta| \simeq 2.1$, with velocities $v_w > 0.4$ being disfavored for those fixed Yukawa couplings and order parameters. Although the plot also appears to indicate that smaller velocities, $v_w < 0.25$, are disfavored, for each scenario we obtain multiple values of v_w , as shown in Fig. 2, and here we simply show the largest of these. Furthermore, since the BAU is predicted to be too large for a significant range of lower v_w there is plenty of scope to adjust parameters so that it agrees with the observed value.

Finally we note that while we are confident that our use of the WKB approach conservatively demonstrates we can obtain a sufficiently large BAU while satisfying EDM limits, the fact that it gives a conservative (under-)estimate of the BAU, in comparison to the VR approach, means that a different BAU calculation may allow for lower bubble wall velocities. Thus care should be taken in inferring any specific bounds from our plots.

Interestingly, sensitivity projections from the future Higgs factories, CEPC [58] and FCC-ee [59] (orange dashed curve), indicate that future experimental studies of Higgs di-tau decay properties sensitive to $\tilde{\kappa}_\tau$ can test our predictions. Specifically, we assume 5 ab^{-1} integrated luminosity to obtain a projected sensitivity to $|\tilde{\kappa}_\tau/\kappa_\tau| \lesssim 0.05$ [81, 100–105] as indicated by the orange dashed curve in Fig. 3. Furthermore, the future sensitivity on the eEDM at the ACME III experiment [88] (cyan dashed curve) indicates it could probe almost all of the parameter space of our current scenario.

Outlook. Our study of EWBG in the G2HDM provides a proof of principle that new physics explaining the $R(D^{(*)})$ anomalies can admit sufficient CP-violation as needed to explain the BAU while respecting eEDM and other phenomenological constraints. To our knowledge, this work represents the first time such a connection between the charged current anomalies and successful EWBG has been demonstrated. Our finding relies on using the WKB method for a conservative estimate of the BAU, while employing a new approach that gives an analytical solution through simplifying approximations. This work can be generalized for more complicated cases using different lepton diffusion constants $D_L \neq D_R$, as well as including quarks in the full transport equations that were updated in Ref. [61]. More complete numerical studies of the G2HDM, including a computation of the BAU in the VR framework, identifying the values

of the scalar potential parameters needed for a SF OPT, and determining their impact on the bubble wall profile and velocity, would yield a more quantitatively robust connection between the BAU and flavor anomalies.

ACKNOWLEDGMENTS

We thank B. Laurent for useful correspondence. We acknowledge the EuroHPC Joint Undertaking for awarding this project access to the EuroHPC supercomputer LUMI, hosted by CSC (Finland) and the LUMI consortium through a EuroHPC Extreme Scale Access call. The work of both PA and CS is supported by the National Natural Science Foundation of China (NNSFC) under grant No. 12150610460. The work of CS is also supported by the Excellent Postdoctoral Program of Jiangsu Province grant No. 2023ZB891 and the work of PA by NNSFC Key Projects grant No. 12335005 and the supporting fund for foreign experts grant wgzx2022021. YW is supported by NNSFC under grant No. 12305112. MJRM is supported in part under NNSFC grant No. 12375094.

* peter.athron@coepp.org.au

† mjrm@sjtu.edu.cn, mjrm@physics.umass.edu

‡ Corresponding author: cristian.sierra@njnu.edu.cn

§ ycwu@njnu.edu.cn

- [1] A. D. Sakharov, Violation of CP Invariance, C asymmetry, and baryon asymmetry of the universe, *Pisma Zh. Eksp. Teor. Fiz.* **5**, 32 (1967).
- [2] V. A. Kuzmin, V. A. Rubakov, and M. E. Shaposhnikov, On the Anomalous Electroweak Baryon Number Non-conservation in the Early Universe, *Phys. Lett. B* **155**, 36 (1985).
- [3] M. E. Shaposhnikov, Possible Appearance of the Baryon Asymmetry of the Universe in an Electroweak Theory, *JETP Lett.* **44**, 465 (1986).
- [4] M. E. Shaposhnikov, Baryon Asymmetry of the Universe in Standard Electroweak Theory, *Nucl. Phys. B* **287**, 757 (1987).
- [5] J. M. Cline, Baryogenesis, in *Les Houches Summer School - Session 86: Particle Physics and Cosmology: The Fabric of Spacetime* (2006) [arXiv:hep-ph/0609145](https://arxiv.org/abs/hep-ph/0609145).
- [6] D. E. Morrissey and M. J. Ramsey-Musolf, Electroweak baryogenesis, *New J. Phys.* **14**, 125003 (2012), [arXiv:1206.2942 \[hep-ph\]](https://arxiv.org/abs/1206.2942).
- [7] T. Chupp, P. Fierlinger, M. Ramsey-Musolf, and J. Singh, Electric dipole moments of atoms, molecules, nuclei, and particles, *Rev. Mod. Phys.* **91**, 015001 (2019), [arXiv:1710.02504 \[physics.atom-ph\]](https://arxiv.org/abs/1710.02504).
- [8] D. Curtin, P. Meade, and C.-T. Yu, Testing Electroweak Baryogenesis with Future Colliders, *JHEP* **11**, 127, [arXiv:1409.0005 \[hep-ph\]](https://arxiv.org/abs/1409.0005).
- [9] M. J. Ramsey-Musolf, The electroweak phase transition: a collider target, *JHEP* **09**, 179, [arXiv:1912.07189 \[hep-ph\]](https://arxiv.org/abs/1912.07189).

- [10] C. Caprini *et al.*, Science with the space-based interferometer eLISA. II: Gravitational waves from cosmological phase transitions, *JCAP* **04**, 001, [arXiv:1512.06239 \[astro-ph.CO\]](#).
- [11] F. P. Huang, Y. Wan, D.-G. Wang, Y.-F. Cai, and X. Zhang, Hearing the echoes of electroweak baryogenesis with gravitational wave detectors, *Phys. Rev. D* **94**, 041702 (2016), [arXiv:1601.01640 \[hep-ph\]](#).
- [12] A. Beniwal, M. Lewicki, J. D. Wells, M. White, and A. G. Williams, Gravitational wave, collider and dark matter signals from a scalar singlet electroweak baryogenesis, *JHEP* **08**, 108, [arXiv:1702.06124 \[hep-ph\]](#).
- [13] N. S. Manton, Topology in the Weinberg-Salam Theory, *Phys. Rev. D* **28**, 2019 (1983).
- [14] F. R. Klinkhamer and N. S. Manton, A Saddle Point Solution in the Weinberg-Salam Theory, *Phys. Rev. D* **30**, 2212 (1984).
- [15] R. Martinez, C. Sierra, and G. Valencia, Beyond $\mathcal{R}(D^{(*)})$ with the general type-III 2HDM for $b \rightarrow c\nu$, *Phys. Rev. D* **98**, 115012 (2018), [arXiv:1805.04098 \[hep-ph\]](#).
- [16] A. Crivellin and S. Iguro, Accumulating hints for flavor-violating Higgs bosons at the electroweak scale, *Phys. Rev. D* **110**, 015014 (2024), [arXiv:2311.03430 \[hep-ph\]](#).
- [17] P. Athron, A. Crivellin, T. E. Gonzalo, S. Iguro, and C. Sierra, Global fit to the 2HDM with generic sources of flavour violation using GAMBIT, *JHEP* **11**, 133, [arXiv:2410.10493 \[hep-ph\]](#).
- [18] Y. S. Amhis *et al.* (HFLAV), Averages of b-hadron, c-hadron, and τ -lepton properties as of 2021, *Phys. Rev. D* **107**, 052008 (2023), [arXiv:2206.07501 \[hep-ex\]](#).
- [19] R. Aaij *et al.* (LHCb), Measurement of CP -Averaged Observables in the $B^0 \rightarrow K^{*0}\mu^+\mu^-$ Decay, *Phys. Rev. Lett.* **125**, 011802 (2020), [arXiv:2003.04831 \[hep-ex\]](#).
- [20] *Angular analysis of the $B^0 \rightarrow K^{*0}(892)\mu^+\mu^-$ decay at $\sqrt{s} = 13$ TeV*, Tech. Rep. (CERN, Geneva, 2024).
- [21] A. Greljo, J. Salko, A. Smolkovič, and P. Stangl, Rare b decays meet high-mass Drell-Yan, *JHEP* **05**, 087, [arXiv:2212.10497 \[hep-ph\]](#).
- [22] M. Algueró, A. Biswas, B. Capdevila, S. Descotes-Genon, J. Matias, and M. Novoa-Brunet, To (b)e or not to (b)e: no electrons at LHCb, *Eur. Phys. J. C* **83**, 648 (2023), [arXiv:2304.07330 \[hep-ph\]](#).
- [23] A. Crivellin and B. Mellado, Anomalies in Particle Physics, *Nature Rev. Phys.* [10.1038/s42254-024-00703-6](#) (2024), [arXiv:2309.03870 \[hep-ph\]](#).
- [24] T. S. Roussy *et al.*, An improved bound on the electron's electric dipole moment, *Science* **381**, adg4084 (2023), [arXiv:2212.11841 \[physics.atom-ph\]](#).
- [25] T. Liu, M. J. Ramsey-Musolf, and J. Shu, Electroweak Beautygenesis: From $b \rightarrow s$ CP-violation to the Cosmic Baryon Asymmetry, *Phys. Rev. Lett.* **108**, 221301 (2012), [arXiv:1109.4145 \[hep-ph\]](#).
- [26] S. Tulin and P. Winslow, Anomalous B meson mixing and baryogenesis, *Phys. Rev. D* **84**, 034013 (2011), [arXiv:1105.2848 \[hep-ph\]](#).
- [27] J. M. Cline, K. Kainulainen, and M. Trott, Electroweak Baryogenesis in Two Higgs Doublet Models and B meson anomalies, *JHEP* **11**, 089, [arXiv:1107.3559 \[hep-ph\]](#).
- [28] A. E. Nelson and H. Xiao, Baryogenesis from B Meson Oscillations, *Phys. Rev. D* **100**, 075002 (2019), [arXiv:1901.08141 \[hep-ph\]](#).
- [29] W.-S. Hou, G. Kumar, and T. Modak, Probing baryogenesis with radiative beauty decay and electron electric dipole moment, *Phys. Rev. D* **109**, L011701 (2024), [arXiv:2302.08847 \[hep-ph\]](#).
- [30] Y.-Z. Li, M. J. Ramsey-Musolf, and J.-H. Yu, Does the Electron EDM Preclude Electroweak Baryogenesis? (2024), [arXiv:2404.19197 \[hep-ph\]](#).
- [31] K. Kajantie, M. Laine, K. Rummukainen, and M. E. Shaposhnikov, Is there a hot electroweak phase transition at $m_H \gtrsim m_W$?, *Phys. Rev. Lett.* **77**, 2887 (1996), [arXiv:hep-ph/9605288](#).
- [32] G. C. Dorsch, S. J. Huber, and J. M. No, A strong electroweak phase transition in the 2HDM after LHC8, *JHEP* **10**, 029, [arXiv:1305.6610 \[hep-ph\]](#).
- [33] P. Basler, M. Krause, M. Muhlleitner, J. Wittbrodt, and A. Wlotzka, Strong First Order Electroweak Phase Transition in the CP-Conserving 2HDM Revisited, *JHEP* **02**, 121, [arXiv:1612.04086 \[hep-ph\]](#).
- [34] J. Bernon, L. Bian, and Y. Jiang, A new insight into the phase transition in the early Universe with two Higgs doublets, *JHEP* **05**, 151, [arXiv:1712.08430 \[hep-ph\]](#).
- [35] G. C. Dorsch, S. J. Huber, K. Mimasu, and J. M. No, The Higgs Vacuum Uplifted: Revisiting the Electroweak Phase Transition with a Second Higgs Doublet, *JHEP* **12**, 086, [arXiv:1705.09186 \[hep-ph\]](#).
- [36] J. O. Andersen, T. Gorda, A. Helset, L. Niemi, T. V. I. Tenkanen, A. Tranberg, A. Vuorinen, and D. J. Weir, Nonperturbative Analysis of the Electroweak Phase Transition in the Two Higgs Doublet Model, *Phys. Rev. Lett.* **121**, 191802 (2018), [arXiv:1711.09849 \[hep-ph\]](#).
- [37] K. Kainulainen, V. Keus, L. Niemi, K. Rummukainen, T. V. I. Tenkanen, and V. Vaskonen, On the validity of perturbative studies of the electroweak phase transition in the Two Higgs Doublet model, *JHEP* **06**, 075, [arXiv:1904.01329 \[hep-ph\]](#).
- [38] W. Su, A. G. Williams, and M. Zhang, Strong first order electroweak phase transition in 2HDM confronting future Z & Higgs factories, *JHEP* **04**, 219, [arXiv:2011.04540 \[hep-ph\]](#).
- [39] D. Gonçalves, A. Kaladharan, and Y. Wu, Electroweak phase transition in the 2HDM: Collider and gravitational wave complementarity, *Phys. Rev. D* **105**, 095041 (2022), [arXiv:2108.05356 \[hep-ph\]](#).
- [40] T. Biekötter, S. Heinemeyer, J. M. No, M. O. Leiaromacho, and G. Weiglein, The trap in the early Universe: impact on the interplay between gravitational waves and LHC physics in the 2HDM, *JCAP* **03**, 031, [arXiv:2208.14466 \[hep-ph\]](#).
- [41] D. Gonçalves, A. Kaladharan, and Y. Wu, Gravitational waves, bubble profile, and baryon asymmetry in the complex 2HDM, *Phys. Rev. D* **108**, 075010 (2023), [arXiv:2307.03224 \[hep-ph\]](#).
- [42] A. G. Cohen, D. B. Kaplan, and A. E. Nelson, Spontaneous baryogenesis at the weak phase transition, *Phys. Lett. B* **263**, 86 (1991).
- [43] M. Joyce, T. Prokopec, and N. Turok, Efficient electroweak baryogenesis from lepton transport, *Phys. Lett. B* **338**, 269 (1994), [arXiv:hep-ph/9401352](#).
- [44] J. M. Cline, K. Kainulainen, and A. P. Vischer, Dynamics of two Higgs doublet CP violation and baryogenesis at the electroweak phase transition, *Phys. Rev. D* **54**, 2451 (1996), [arXiv:hep-ph/9506284](#).
- [45] L. Fromme, S. J. Huber, and M. Seniuch, Baryogenesis in the two-Higgs doublet model, *JHEP* **11**, 038,

- arXiv:hep-ph/0605242.
- [46] L. Fromme and S. J. Huber, Top transport in electroweak baryogenesis, *JHEP* **03**, 049, arXiv:hep-ph/0604159.
- [47] V. Cirigliano, Y. Li, S. Profumo, and M. J. Ramsey-Musolf, MSSM Baryogenesis and Electric Dipole Moments: An Update on the Phenomenology, *JHEP* **01**, 002, arXiv:0910.4589 [hep-ph].
- [48] G. C. Dorsch, S. J. Huber, T. Konstandin, and J. M. No, A Second Higgs Doublet in the Early Universe: Baryogenesis and Gravitational Waves, *JCAP* **05**, 052, arXiv:1611.05874 [hep-ph].
- [49] P. Basler, L. Biermann, M. Mühlleitner, and J. Müller, Electroweak baryogenesis in the CP-violating two-Higgs doublet model, *Eur. Phys. J. C* **83**, 57 (2023), arXiv:2108.03580 [hep-ph].
- [50] K. Enomoto, S. Kanemura, and Y. Mura, Electroweak baryogenesis in aligned two Higgs doublet models, *JHEP* **01**, 104, arXiv:2111.13079 [hep-ph].
- [51] K. Enomoto, S. Kanemura, and Y. Mura, New benchmark scenarios of electroweak baryogenesis in aligned two Higgs double models, *JHEP* **09**, 121, arXiv:2207.00060 [hep-ph].
- [52] D. J. H. Chung, B. Garbrecht, M. J. Ramsey-Musolf, and S. Tulin, Yukawa Interactions and Supersymmetric Electroweak Baryogenesis, *Phys. Rev. Lett.* **102**, 061301 (2009), arXiv:0808.1144 [hep-ph].
- [53] D. J. H. Chung, B. Garbrecht, M. J. Ramsey-Musolf, and S. Tulin, Lepton-mediated electroweak baryogenesis, *Phys. Rev. D* **81**, 063506 (2010), arXiv:0905.4509 [hep-ph].
- [54] H.-K. Guo, Y.-Y. Li, T. Liu, M. Ramsey-Musolf, and J. Shu, Lepton-Flavored Electroweak Baryogenesis, *Phys. Rev. D* **96**, 115034 (2017), arXiv:1609.09849 [hep-ph].
- [55] C.-W. Chiang, K. Fuyuto, and E. Senaha, Electroweak Baryogenesis with Lepton Flavor Violation, *Phys. Lett. B* **762**, 315 (2016), arXiv:1607.07316 [hep-ph].
- [56] K. Fuyuto, W.-S. Hou, and E. Senaha, Electroweak baryogenesis driven by extra top Yukawa couplings, *Phys. Lett. B* **776**, 402 (2018), arXiv:1705.05034 [hep-ph].
- [57] G. Aad *et al.* (ATLAS), Search for a light charged Higgs boson in $t \rightarrow H^\pm b$ decays, with $H^\pm \rightarrow cb$, in the lepton+jets final state in proton-proton collisions at $\sqrt{s} = 13$ TeV with the ATLAS detector, *JHEP* **09**, 004, arXiv:2302.11739 [hep-ex].
- [58] M. Dong *et al.* (CEPC Study Group), CEPC Conceptual Design Report: Volume 2 - Physics & Detector (2018), arXiv:1811.10545 [hep-ex].
- [59] A. Abada *et al.* (FCC), FCC-ee: The Lepton Collider: Future Circular Collider Conceptual Design Report Volume 2, *Eur. Phys. J. ST* **228**, 261 (2019).
- [60] J. M. Cline, M. Joyce, and K. Kainulainen, Supersymmetric electroweak baryogenesis, *JHEP* **07**, 018, arXiv:hep-ph/0006119.
- [61] J. M. Cline and K. Kainulainen, Electroweak baryogenesis at high bubble wall velocities, *Phys. Rev. D* **101**, 063525 (2020), arXiv:2001.00568 [hep-ph].
- [62] K. Kainulainen, CP-violating transport theory for electroweak baryogenesis with thermal corrections, *JCAP* **11** (11), 042, arXiv:2108.08336 [hep-ph].
- [63] J. De Vries, M. Postma, and J. van de Vis, The role of leptons in electroweak baryogenesis, *JHEP* **04**, 024, arXiv:1811.11104 [hep-ph].
- [64] V. Cirigliano, C. Lee, M. J. Ramsey-Musolf, and S. Tulin, Flavored Quantum Boltzmann Equations, *Phys. Rev. D* **81**, 103503 (2010), arXiv:0912.3523 [hep-ph].
- [65] V. Cirigliano, C. Lee, and S. Tulin, Resonant Flavor Oscillations in Electroweak Baryogenesis, *Phys. Rev. D* **84**, 056006 (2011), arXiv:1106.0747 [hep-ph].
- [66] P. Huet and A. E. Nelson, Electroweak baryogenesis in supersymmetric models, *Phys. Rev. D* **53**, 4578 (1996), arXiv:hep-ph/9506477.
- [67] C. Lee, V. Cirigliano, and M. J. Ramsey-Musolf, Resonant relaxation in electroweak baryogenesis, *Phys. Rev. D* **71**, 075010 (2005), arXiv:hep-ph/0412354.
- [68] V. Cirigliano, M. J. Ramsey-Musolf, S. Tulin, and C. Lee, Yukawa and tri-scalar processes in electroweak baryogenesis, *Phys. Rev. D* **73**, 115009 (2006), arXiv:hep-ph/0603058.
- [69] K.-P. Xie, Lepton-mediated electroweak baryogenesis, gravitational waves and the 4τ final state at the collider, *JHEP* **02**, 090, [Erratum: *JHEP* 8, 052 (2022)], arXiv:2011.04821 [hep-ph].
- [70] A. G. Cohen, D. B. Kaplan, and A. E. Nelson, Diffusion enhances spontaneous electroweak baryogenesis, *Phys. Lett. B* **336**, 41 (1994), arXiv:hep-ph/9406345.
- [71] J. M. Cline and B. Laurent, Electroweak baryogenesis from light fermion sources: A critical study, *Phys. Rev. D* **104**, 083507 (2021), arXiv:2108.04249 [hep-ph].
- [72] P. B. Arnold, G. D. Moore, and L. G. Yaffe, Transport coefficients in high temperature gauge theories. I. Leading log results, *JHEP* **11**, 001, arXiv:hep-ph/0010177.
- [73] “Preliminary average of $R(D)$ and $R(D^*)$ for Moriond 2024” at <https://hflav-eos.web.cern.ch/hflav-eos/semi/moriond24/html/RDsDstar/RDRDs.html>.
- [74] G. M. de Divitiis, R. Petronzio, and N. Tantalo, Quenched lattice calculation of semileptonic heavy-light meson form factors, *JHEP* **10**, 062, arXiv:0707.0587 [hep-lat].
- [75] J. F. Kamenik and F. Mescia, $B \rightarrow D\tau\nu$ Branching Ratios: Opportunity for Lattice QCD and Hadron Colliders, *Phys. Rev. D* **78**, 014003 (2008), arXiv:0802.3790 [hep-ph].
- [76] F. Mahmoudi, SuperIso: A Program for calculating the isospin asymmetry of $B \rightarrow K^* \gamma$ in the MSSM, *Comput. Phys. Commun.* **178**, 745 (2008), arXiv:0710.2067 [hep-ph].
- [77] F. Mahmoudi, SuperIso v2.3: A Program for calculating flavor physics observables in Supersymmetry, *Comput. Phys. Commun.* **180**, 1579 (2009), arXiv:0808.3144 [hep-ph].
- [78] F. Mahmoudi, SuperIso v3.0, flavor physics observables calculations: Extension to NMSSM, *Comput. Phys. Commun.* **180**, 1718 (2009).
- [79] P. Athron, C. Balazs, T. E. Gonzalo, D. Jacob, F. Mahmoudi, and C. Sierra, Likelihood analysis of the flavour anomalies and $g - 2$ in the general two Higgs doublet model, *JHEP* **01**, 037, arXiv:2111.10464 [hep-ph].
- [80] J. Alonso-González, L. Merlo, and S. Pokorski, A new bound on CP violation in the τ lepton Yukawa coupling and electroweak baryogenesis, *JHEP* **06**, 166, arXiv:2103.16569 [hep-ph].
- [81] S.-F. Ge, G. Li, P. Pasquini, and M. J. Ramsey-Musolf, CP-violating Higgs Di-tau Decays: Baryogenesis and

- Higgs Factories, *Phys. Rev. D* **103**, 095027 (2021), [arXiv:2012.13922 \[hep-ph\]](#).
- [82] J. Hisano, K. Tsumura, and M. J. S. Yang, QCD Corrections to Neutron Electric Dipole Moment from Dimension-six Four-Quark Operators, *Phys. Lett. B* **713**, 473 (2012), [arXiv:1205.2212 \[hep-ph\]](#).
- [83] J. Hisano, J. Y. Lee, N. Nagata, and Y. Shimizu, Reevaluation of Neutron Electric Dipole Moment with QCD Sum Rules, *Phys. Rev. D* **85**, 114044 (2012), [arXiv:1204.2653 \[hep-ph\]](#).
- [84] J. Engel, M. J. Ramsey-Musolf, and U. van Kolck, Electric Dipole Moments of Nucleons, Nuclei, and Atoms: The Standard Model and Beyond, *Prog. Part. Nucl. Phys.* **71**, 21 (2013), [arXiv:1303.2371 \[nucl-th\]](#).
- [85] S. Bertolini, A. Maiezza, and F. Nesti, Kaon CP violation and neutron EDM in the minimal left-right symmetric model, *Phys. Rev. D* **101**, 035036 (2020), [arXiv:1911.09472 \[hep-ph\]](#).
- [86] C. Abel *et al.*, Measurement of the Permanent Electric Dipole Moment of the Neutron, *Phys. Rev. Lett.* **124**, 081803 (2020), [arXiv:2001.11966 \[hep-ex\]](#).
- [87] E. Fuchs, M. Losada, Y. Nir, and Y. Viernik, CP violation from τ , t and b dimension-6 Yukawa couplings - interplay of baryogenesis, EDM and Higgs physics, *JHEP* **05**, 056, [arXiv:2003.00099 \[hep-ph\]](#).
- [88] D. G. Ang, *Progress towards an improved measurement of the electric dipole moment of the electron*, Ph.D. thesis, Harvard U. (2023).
- [89] S. Kanemura and Y. Mura, Electroweak baryogenesis via top-charm mixing, *JHEP* **09**, 153, [arXiv:2303.11252 \[hep-ph\]](#).
- [90] S. Navas *et al.* (Particle Data Group), Review of particle physics, *Phys. Rev. D* **110**, 030001 (2024).
- [91] P. Athron *et al.* (GAMBIT Collaboration), GAMBIT: The Global and Modular Beyond-the-Standard-Model Inference Tool, *Eur. Phys. J. C* **77**, 784 (2017), [Addendum: *Eur.Phys.J.C* 78, 98 (2018).], [arXiv:1705.07908 \[hep-ph\]](#).
- [92] G. D. Martinez, J. McKay, B. Farmer, P. Scott, E. Roebber, A. Putze, and J. Conrad (GAMBIT), Comparison of statistical sampling methods with ScannerBit, the GAMBIT scanning module, *Eur. Phys. J. C* **77**, 761 (2017), [arXiv:1705.07959 \[hep-ph\]](#).
- [93] F. U. Bernlochner *et al.* (GAMBIT Flavour Workgroup), FlavBit: A GAMBIT module for computing flavour observables and likelihoods, *Eur. Phys. J. C* **77**, 786 (2017), [arXiv:1705.07933 \[hep-ph\]](#).
- [94] P. Athron *et al.* (GAMBIT Models Workgroup), SpecBit, DecayBit and PrecisionBit: GAMBIT modules for computing mass spectra, particle decay rates and precision observables, *Eur. Phys. J. C* **78**, 22 (2018), [arXiv:1705.07936 \[hep-ph\]](#).
- [95] C. Balázs *et al.* (GAMBIT), ColliderBit: a GAMBIT module for the calculation of high-energy collider observables and likelihoods, *Eur. Phys. J. C* **77**, 795 (2017), [arXiv:1705.07919 \[hep-ph\]](#).
- [96] D. Eriksson, J. Rathsman, and O. Stal, 2HDMC: Two-Higgs-Doublet Model Calculator Physics and Manual, *Comput. Phys. Commun.* **181**, 189 (2010), [arXiv:0902.0851 \[hep-ph\]](#).
- [97] J. Bhom and M. Chrzaszcz, HEPLike: an open source framework for experimental likelihood evaluation, *Comput. Phys. Commun.* **254**, 107235 (2020), [arXiv:2003.03956 \[physics.data-an\]](#).
- [98] P. A. R. Ade *et al.* (Planck), Planck 2013 results. XVI. Cosmological parameters, *Astron. Astrophys.* **571**, A16 (2014), [arXiv:1303.5076 \[astro-ph.CO\]](#).
- [99] M. Blanke, A. Crivellin, S. de Boer, T. Kitahara, M. Moscati, U. Nierste, and I. Nišandžić, Impact of polarization observables and $B_c \rightarrow \tau\nu$ on new physics explanations of the $b \rightarrow c\tau\nu$ anomaly, *Phys. Rev. D* **99**, 075006 (2019), [arXiv:1811.09603 \[hep-ph\]](#).
- [100] X. Chen and Y. Wu, Search for CP violation effects in the $h \rightarrow \tau\tau$ decay with e^+e^- colliders, *Eur. Phys. J. C* **77**, 697 (2017), [arXiv:1703.04855 \[hep-ph\]](#).
- [101] X. Chen and Y. Wu, Probing the CP-Violation effects in the $h\tau\tau$ coupling at the LHC, *Phys. Lett. B* **790**, 332 (2019), [arXiv:1708.02882 \[hep-ph\]](#).
- [102] D. Jeans and G. W. Wilson, Measuring the CP state of tau lepton pairs from Higgs decay at the ILC, *Phys. Rev. D* **98**, 013007 (2018), [arXiv:1804.01241 \[hep-ex\]](#).
- [103] M. M. Altakach, P. Lamba, F. Maltoni, K. Mawatari, and K. Sakurai, Quantum information and CP measurement in $H \rightarrow \tau^+\tau^-$ at future lepton colliders, *Phys. Rev. D* **107**, 093002 (2023), [arXiv:2211.10513 \[hep-ph\]](#).
- [104] A. V. Gritsan *et al.*, Snowmass White Paper: Prospects of CP-violation measurements with the Higgs boson at future experiments (2022), [arXiv:2205.07715 \[hep-ex\]](#).
- [105] A. Aryshev *et al.* (ILC International Development Team), The International Linear Collider: Report to Snowmass 2021 (2022), [arXiv:2203.07622 \[physics.acc-ph\]](#).
- [106] J. de Vries, M. Postma, J. van de Vis, and G. White, Electroweak Baryogenesis and the Standard Model Effective Field Theory, *JHEP* **01**, 089, [arXiv:1710.04061 \[hep-ph\]](#).
- [107] M. Postma and J. van de Vis, Source terms for electroweak baryogenesis in the vev-insertion approximation beyond leading order, *JHEP* **02**, 090, [arXiv:1910.11794 \[hep-ph\]](#).
- [108] P. Elmfors, K. Enqvist, A. Riotto, and I. Vilja, Damping rates in the MSSM and electroweak baryogenesis, *Phys. Lett. B* **452**, 279 (1999), [arXiv:hep-ph/9809529](#).
- [109] J. Herrero-Garcia, M. Nebot, F. Rajec, M. White, and A. G. Williams, Higgs Quark Flavor Violation: Simplified Models and Status of General Two-Higgs-Doublet Model, *JHEP* **02**, 147, [arXiv:1907.05900 \[hep-ph\]](#).
- [110] J. M. Moreno, M. Quiros, and M. Seco, Bubbles in the supersymmetric standard model, *Nucl. Phys. B* **526**, 489 (1998), [arXiv:hep-ph/9801272](#).
- [111] K. Funakubo and E. Senaha, Electroweak phase transition, critical bubbles and sphaleron decoupling condition in the MSSM, *Phys. Rev. D* **79**, 115024 (2009), [arXiv:0905.2022 \[hep-ph\]](#).
- [112] K. Kainulainen, T. Prokopec, M. G. Schmidt, and S. Weinstock, Semiclassical force for electroweak baryogenesis: Three-dimensional derivation, *Phys. Rev. D* **66**, 043502 (2002), [arXiv:hep-ph/0202177](#).
- [113] C. Jarlskog, Commutator of the Quark Mass Matrices in the Standard Electroweak Model and a Measure of Maximal CP Nonconservation, *Phys. Rev. Lett.* **55**, 1039 (1985).
- [114] F. J. Botella and J. P. Silva, Jarlskog - like invariants for theories with scalars and fermions, *Phys. Rev. D* **51**, 3870 (1995), [arXiv:hep-ph/9411288](#).

End Matter

Diffusion equation. The explicit coefficients and source term of the diffusion equation in Eq.(1) are given by

$$\begin{aligned}\bar{D}_l &= \frac{-D_2 + D_0 v_w^2}{\Gamma_{\text{tot},l} D_0}, \\ \bar{\Gamma}_l &= k_l \frac{K_0}{D_0} \Gamma_{\text{eff}}, \\ \bar{S}_l &= -k_l \frac{T^2}{6} \left(\frac{S_1}{D_0} + \frac{v_w S'_1 - S'_2}{\Gamma_{\text{tot},l} D_0} \right),\end{aligned}\quad (\text{A1})$$

where $K_0 \simeq 1.1$ for all bubble wall velocities and temperatures in the massless case. As shown in Ref. [67], the statistical k_l factors are in general functions of the thermal masses which for chiral leptons are well approximated by the massless case, i.e., $k_L(0) = 2$ and $k_R(0) = 1$ obtained when assuming local thermal equilibrium and expanding the number densities l in small chemical potentials $\mu_l = (1/k_l)(6/T^2)l$.

The general expressions for the source functions $S_{1,2}$ in Eq.(A1) are given in Ref. [61] and will depend on the model being considered. The total interaction rate $\Gamma_{\text{tot},l}$ is defined as

$$\Gamma_{\text{tot},l} = \frac{D_2(v_w)}{D_0 D_l}, \quad (\text{A2})$$

with $D_0 = 1$ and

$$D_2(v_w) = \frac{v_w (2v_w^2 - 1) + (v_w^2 - 1)^2 \tanh^{-1} v_w}{v_w^3}, \quad (\text{A3})$$

both for massless fermions as well, and D_l the lepton's diffusion constant. The different signs in Eq.(A1) with respect to the results obtained in Ref. [61] come from having the expanding wall going to the left which means $v_w \rightarrow -v_w$.

The effective relaxation rate from inelastic scattering between leptons and the bubble wall is,

$$\Gamma_{\text{eff}} \equiv \left(\frac{1}{k_L} + \frac{1}{k_R} \right) (\Gamma_{m_\tau} + \Gamma_{Y_\tau}), \quad (\text{A4})$$

with $\Gamma_{Y_\tau} = 4.4 \times 10^{-7} T$ [71] and we calculate Γ_{m_τ} from [106, 107] obtaining $\Gamma_{m_\tau} = 0.3 m_\tau^2/T$, where we have estimated the damping rate for the τ lepton as $\gamma_\tau \simeq 0.025 T$ from [108] as in the case of Higgsinos.

The amplitude \mathcal{A} in Eq.(2) is expressed as

$$\begin{aligned}\mathcal{A} &= \int_0^\infty dy \bar{S}_l(y) \frac{e^{-\gamma_+^b y}}{D_l (\gamma_+^b - \gamma_-^s)} \\ &+ \int_{-L_w/2}^0 dy \bar{S}_l(y) \left[\frac{\gamma_-^b}{v_w \gamma_+^b} + \frac{e^{-v_w y/\bar{D}_l}}{v_w} \right],\end{aligned}\quad (\text{A5})$$

where it is understood that we are approximating the collision rate as a step function $\Gamma_{\text{eff}} = \Gamma_{\text{eff}} H(z)$ and γ_\pm are the solutions of the auxiliary equation of the homogeneous case for Eq.(1), $\gamma_\pm = 1/2\bar{D}_l (v_w \pm \sqrt{v_w^2 + 4\bar{\Gamma}_l \bar{D}_l})$, with the b and s notations referring to the *broken* and *symmetric* phases respectively.

Yukawa Lagrangian. The most general Yukawa Lagrangian for leptons in the generic scalar basis $\{\Phi_1, \Phi_2\}$ for the G2HDM reads [109]:

$$-\mathcal{L}_Y = \bar{L}_L^0 (\tilde{Y}_1^1 \Phi_1 + \tilde{Y}_1^2 \Phi_2) l_R^0 + \text{h.c.}, \quad (\text{B1})$$

with $L = (\nu_l, l)^T$ and the “0” notation refers to the flavor eigenstates. The charged lepton masses are

$$M_l = \frac{1}{\sqrt{2}} (v_1 \tilde{Y}_l^1 + v_2 \tilde{Y}_l^2), \quad (\text{B2})$$

with v_1 and v_2 the VEVs of Φ_1 and Φ_2 respectively at zero temperature and $v = \sqrt{v_1^2 + v_2^2} = 246.22 \text{ GeV}$. Eq.(B2) is diagonalized through a bi-unitary transformation $\bar{M}_l = V_{lL}^\dagger M_l V_{lR}$ where the fact that M_l is Hermitian implies that $\bar{V}_l \equiv V_{lL} = V_{lR}$, and the mass eigenstates for the charged leptons are given by $l = V_l^\dagger l^0$. In this way, Eq.(B2) takes the form $\bar{M}_l = 1/\sqrt{2}(v_1 Y_l^1 + v_2 Y_l^2)$ where $Y_l^i = V_{lL}^\dagger \tilde{Y}_l^i V_{lR}$, diagonalizing then the charged lepton mass matrix. Using these expressions, we can write the Yukawa Lagrangian in the mass basis as,

$$-\mathcal{L}_Y = \bar{\nu}_b \rho_\ell^{ba} P_R l_a H^+ + \sum_\phi \bar{l}_b \Gamma_l^{\phi ba} P_R l_a \phi + \text{h.c.}, \quad (\text{B3})$$

for $\phi = h, H, A$, here a, b are explicit flavor indices and

$$\begin{aligned}\rho_l^{ba} &\equiv \frac{Y_l^{2,ba}}{\cos \beta} - \frac{\sqrt{2} \tan \beta \bar{M}_l^{ba}}{v}, \\ \Gamma_l^{hba} &\equiv \frac{\bar{M}_l^{ba}}{v} s_{\beta-\alpha} + \frac{1}{\sqrt{2}} \rho_l^{ba} c_{\beta-\alpha}, \\ \Gamma_l^{Hba} &\equiv \frac{\bar{M}_l^{ba}}{v} c_{\beta-\alpha} - \frac{1}{\sqrt{2}} \rho_l^{ba} s_{\beta-\alpha}, \\ \Gamma_l^{Aba} &\equiv \frac{i}{\sqrt{2}} \rho_l^{ba},\end{aligned}\quad (\text{B4})$$

with $\tan \beta \equiv v_2/v_1$ at zero temperature and $\beta - \alpha$ is the mixing angle between the CP-even Higgs mass eigenstates h, H relative to the Higgs basis.

Source term in the G2HDM. We use the kink profiles for the two Higgs fields in the bubble wall [71] defined by,

$$\begin{aligned}h_1(z) &= \frac{v_n \cos \beta}{2} \left[1 + \tanh \left(\frac{z}{L_w} \right) \right], \\ h_2(z) &= \frac{v_n \sin \beta}{2} \left[1 + \tanh \left(\frac{z}{L_w} - \Delta\beta \right) \right],\end{aligned}\quad (\text{C1})$$

where v_n is the VEV at the nucleation temperature T_n and $\Delta\beta$ is defined as the maximum variation of β as a

function of z [110, 111]. The tunneling profiles at T_n can also be used, introducing deviations relative to Eqs.(C1) though minor for most cases [41], especially when not considering CP-violation from the scalar sector. We consider the source of CP violation necessary for generating the BAU coming from the Yukawa lepton sector instead and promote the lepton mass matrix in the weak basis in Eq.(B2) to be z -dependent. We use a texture similar to the one implemented in the quark sector in [71] and set,

$$M_l(z) = \frac{1}{\sqrt{2}} \left[\begin{pmatrix} y_{\mu\mu} & y_{\mu\tau} \\ 0 & y_{\tau\tau} \end{pmatrix} h_1 + \begin{pmatrix} y_{\mu\mu} & y_{\mu\tau} \\ 0 & y_{\tau\tau} e^{i\theta} \end{pmatrix} h_2 \right], \quad (\text{C2})$$

with $Y_l^{2,ij} = y_{ij} e^{i\theta_{ij}}$. The texture in Eq.(C2) is also used in [16, 17] with an extra $y_{e\tau}$ coupling which does not affect significantly the $R(D^{(*)})$ ratios.

Identically to Refs. [71, 112] in the case of charginos, in order to calculate the matrix $A = U M_l \partial_z M_l^{-1} U^\dagger$, we diagonalize the $M_l^\dagger M_l$ matrix by the unitary transformation U [60],

$$U = \frac{\sqrt{2}}{\sqrt{\Lambda(\Lambda + \Delta)}} \begin{pmatrix} \frac{1}{2}(\Lambda + \Delta) & a \\ -a^* & \frac{1}{2}(\Lambda + \Delta) \end{pmatrix}, \quad (\text{C3})$$

for $\Delta = (M_l^\dagger M_l)_{11} - (M_l^\dagger M_l)_{22}$, $a = (M_l^\dagger M_l)_{12}$ and $\Lambda = \sqrt{\Delta^2 + 4|a|^2}$. Expanding in small $y_{\mu\mu}$ and $y_{\mu\tau}$ Yukawa couplings, the A_{22} matrix element corresponding to the

heaviest eigenstate is then,

$$A_{22} = \frac{1}{m_+^2} \frac{y_{\mu\tau}^2}{y_{\tau\tau}^2} \frac{(h_1 + h_2)^2 (h_1' h_2 - h_2' h_1) J_A}{2(h_1^2 + h_2^2 + 2h_1 h_2 \cos \theta)}, \quad (\text{C4})$$

where m_+^2 is the corresponding heaviest eigenvalue of $M_l^\dagger M_l$ and J_A is the Jarlskog invariant [54, 113, 114],

$$J_A = \frac{1}{v^2 \mu_{12}^{\text{HB}}} \sum_{a,b,c=1}^2 v_a v_b^* \mu_{bc} \text{Tr}[Y_c Y_a^\dagger], \quad (\text{C5})$$

where μ_{ab} is the coefficient of the $\Phi_a \Phi_b$ term in the Higgs potential as defined in [54] and μ_{12}^{HB} is defined in the Higgs basis. In this way, we find for the source term,

$$S_j = -v_w \gamma_w Q_j^{8o} (m_+^2 \text{Im}(A_{22}))', \quad j = 1, 2, \quad (\text{C6})$$

with $\text{Im}(J_A) = y_{\tau\tau}^2 \sin \theta$ for the Yukawa textures in Eq.(C2), γ_w is the relativistic Lorentz factor and the functions $Q_{1,2}^{8o}$ are given in the massless case by

$$Q_1^{8o} = \frac{3}{4\pi^2 T^2 \gamma_w^2} \ln \left(\frac{v_w - 1}{v_w + 1} \right),$$

$$Q_2^{8o} = \frac{3}{2\pi^2 v_w T^2 \gamma_w^2} \tanh^{-1} v_w. \quad (\text{C7})$$

As in Ref. [71], we have also neglected the contribution proportional to Q_j^{9o} in Eq.(C6) which we have corroborated to be subdominant.